A near-singular, flexure jointed, moment sensitive Stewart platform based force-torque sensor

Shivanand Bhavikatti[1], R. Ranganath[2*] and A. Ghosal[3]
[1,3] Indian Institute of Science, Bangalore-560012, India,
[2] Dynamics & Analysis Division, Spacecraft Mechanisms Group, ISRO Satellite Centre, Bangalore-560017, India,
[*] Corresponding author: - rrrr@isac.gov.in , ranganath_61@yahoo.co.in

Abstract

A force-torque sensor capable of accurate measurement of the three components of externally applied forces and moments is required for force control in robotic applications involving assembly operations. The goal in this paper is to design a Stewart platform based force-torque sensor at a near-singular configuration sensitive to externally applied moments. In such a configuration, we show an enhanced mechanical amplification of leg forces and thereby higher sensitivity for the applied external moments. In other directions, the sensitivity will be that of a normal load sensor determined by the sensitivity of the sensing element and the associated electronic amplification, and all the six components of the force and torque can be sensed.

In a sensor application, the friction, backlash and other non-linearities at the passive spherical joints of the Stewart platform will affect the measurements in unpredictable ways. In this sensor, we use flexural hinges at the leg interfaces of the base and platform of the sensor. The design dimensions of the flexure joints in the sensor have been arrived at using FEA.

The sensor has been fabricated, assembled and instrumented. It has been calibrated for low level loads and is found to show linearity and marked sensitivity to moments about the three orthogonal X, Y and Z axes. This sensor is compatible for usage as a wrist sensor for a robot under development at ISRO Satellite Centre.

Key words: Stewart platform sensor, near-singular, flexure joints

1 Introduction

A six-component force-torque sensor is useful in aerospace applications such as in the measurement of contact forces and moments in space docking and measurement of lift, drag and other quantities in a wind tunnel. A considerable amount of literature exists on the design of force-torque sensor (Gorinevsky et al[1]) and the references listed in them. The original proposal of using a Stewart platform for a flight simulator by Stewart [2] has been followed by its use in a variety of applications including a six component force-torque sensor. This is due to its inherent advantages of being a parallel device (see, for example, Gaillet and Reboulet[3], Dwarakanath et al.[4], M. Prashant et al.[9], Sorli and Pastorelli [10], Champagne et. al., [11], Fichter [12] and McInroy and Hamaan [13].

The idea of mechanical amplification at a near-singular configuration was first used by Ranganath et. al [5] to design and develop a Stewart platform based force-torque sensor with flexure joints having enhanced sensitivity to forces in the horizontal plane and moment about the vertical direction. The goal in this paper is to demonstrate experimentally the sensitivity of a different configuration of a Stewart platform based force-torque sensor with flexure joints at a near-singular configuration to externally applied moments. In such a configuration, we obtain enhanced mechanical amplification of leg forces and thereby higher sensitivity for the applied external moments. In other directions, the sensitivity will be that of a normal load sensor determined by the sensitivity of the sensing element and the associated electronic amplification, thus enabling the sensing of all the six components of force and torque.

2 Choice of singular configuration

The Stewart platform, as shown by a line diagram in Fig. 1, consists of six extensible legs (with prismatic joints in each leg) connected to the (moving) top platform and (fixed) base with spherical(S) joint and Hook(U) joints respectively. As a manipulator, the Stewart platform has six degrees-of-freedom - by actuating the six legs, arbitrary position and orientation of the moving platform can be achieved. If an external force-moment is applied at the top platform, we can obtain the axial forces in the legs required to keep the Stewart platform in equilibrium (see, for example, Dasgupta [7] for details).

The relationship between the six leg forces and the external applied force **F** and moment **M** is given by the matrix equation,

$$(\mathbf{F};\mathbf{M})^T=[H]\,\mathbf{f} \qquad (1)$$

where the 6 x 6 [H] matrix is made up of the unit vectors along the legs and the moment of these unit vectors from the origin of the fixed coordinate system located at the centre of the fixed platform. Denoting the leg unit vectors by $\mathbf{s}_i$, i=1,..., 6 and the moments by $\mathbf{b}_i \times \mathbf{s}_i$, i=1,...,6, the [H] matrix is given as

$[H]= [(\mathbf{s}_1; \mathbf{b}_1 \times \mathbf{s}_1)^T \mid ....|(\mathbf{s}_6; \mathbf{b}_6 \times \mathbf{s}_6)^T]$ (2)
where i^{th} column of [H] is the 6 x 1 entity $(\mathbf{s}_i; \mathbf{b}_i \times \mathbf{s}_i)^T$.

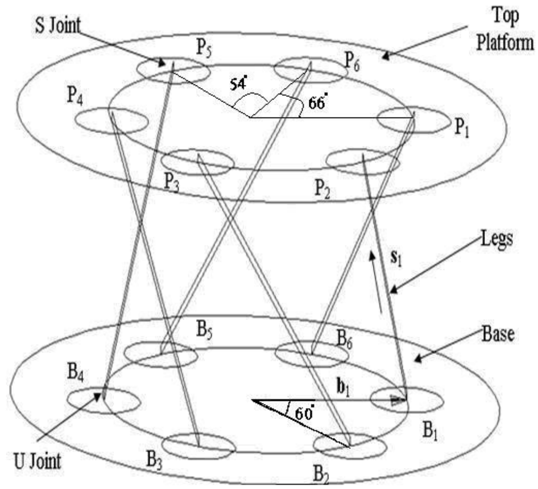

Fig 1a – Line diagram of a 6-6 Stewart platform based Sensor

The matrix [H] is called the force transformation matrix and maps leg forces to externally applied force and moment. If the matrix [H] is singular, some component(s) of the externally applied **F** and **M** cannot be supported by the structure of the Stewart platform obtained by locking the prismatic joints. The structure in such a case gains one or more degrees of freedom instantaneously. The eigenvectors corresponding to the zero eigenvalues of [H] when mapped to 3D space give the singular directions, and the Stewart platform cannot withstand any force/moment applied along the singular directions. If the Stewart platform is in a near-singular configuration, then a small non-zero force/moment acting along the singular direction will lead to large axial force in one or more of the legs, and we will get large magnification. This key concept is utilized in the design of the force-torque sensor in this paper.

From equation (1) and (2), the external force, **F**, can be written as

$$\mathbf{F}= [H_f]\,\mathbf{f} = (\mathbf{s}_1 \mid \mathbf{s}_2| ...| \mathbf{s}_6)\,\mathbf{f} \quad (3)$$

The square of the magnitude of **F** is given by

$$\mathbf{F}^T\mathbf{F}= \mathbf{f}^T [g_f]\;\mathbf{f} \quad (4)$$

and the maximum, intermediate and minimum values of $\mathbf{F}^T\mathbf{F}$ subject to a constraint of the form $\mathbf{f}^T\mathbf{f}=1$ are the eigenvalues of $[g_f]$. Since the rank of $[g_f]$ is 3 ($[H_f]$ has at most rank 3), we can show that the tip of the force vector, **F** lies on an ellipsoid in 3D space. The axes of the ellipsoid are along the *principal forces* and these can be obtained by mapping the eigenvectors corresponding to the non-zero eigenvalues of $[g_f]$ by [H].

Since $[g_f]$ has maximum rank 3, three eigenvalues are always zero and the eigenvectors corresponding to these zero eigenvalues when mapped by [H] give the *principal moments* at the origin. If the rank of $[g_f]$ is less than three, the force ellipsoid shrinks to an ellipse, a line or a point. The singular directions of force can be obtained by mapping the eigenvectors corresponding to the extra zero eigenvalues of $[g_f]$. Likewise the singular direction of the moments is the null space of the matrix obtained from the principal moments.

Using the above procedure, several 6-6 Stewart platform configurations, with equal sized hexagonal base and platform have been investigated by changing the connection sequence between the base and platform points. For several singular configurations, the directions of singularity are also tabulated in Ranganath[5,8]. One among the singular configurations, the connection sequence $\mathbf{B_1}$-$\mathbf{P_2}$, $\mathbf{B_2}$-$\mathbf{P_3}$, $\mathbf{B_3}$-$\mathbf{P_4}$, $\mathbf{B_4}$-$\mathbf{P_5}$, $\mathbf{B_5}$-$\mathbf{P_6}$, $\mathbf{B_6}$-$\mathbf{P_1}$ as seen in Fig.1a has singular directions along the three components of the externally applied moment **M**. Hence, a Stewart platform in a near-singular configuration for this sequence will posses enhanced sensitivity to M_x, M_y, and M_z. This configuration has been chosen for detailed analysis and design, and is shown as a line diagram in Fig.1a.

3 Choice of Sensor Configuration

As mentioned in Section 2, a Stewart platform in a near-singular configuration with $\mathbf{B_1}$-$\mathbf{P_2}$, $\mathbf{B_2}$-$\mathbf{P_3}$, $\mathbf{B_3}$-$\mathbf{P_4}$, $\mathbf{B_4}$-$\mathbf{P_5}$, $\mathbf{B_5}$-$\mathbf{P_6}$, $\mathbf{B_6}$-$\mathbf{P_1}$ was chosen as the leg connection sequence. From the size specifications given by ISRO (shown in Table. 3), the nominal coordinates of the base (as in Table. 1) and platform connection points (as in Table 2) are obtained. The MATLAB simulations for leg forces, assuming spherical joints for the legs at the base and platform, showed considerable leg forces and shown in Fig. 1b. It is seen that the leg forces increase in a non-linear manner with the variation in the platform half angle. The configurations in which the platform points are 3 degrees away from the singular configuration are chosen. This corresponds to 30-33 angle combination, where 30 degrees is the half angle between the two base points and 33 degrees is the half angle between the two platform points. To make the platform a regular hexagon, the alternate half angles are 33 and 27 degrees in the platform, which correspond to 66 and 54 degrees full angle between the adjacent connection points, which is shown in Fig. 1a.

Table 1: Co-ordinates of Base connection points

BASE	X	Y	Z
B_1	25.00	0.00	0
B_2	12.50	21.65	0
B_3	-12.50	21.65	0
B_4	-25.00	0.00	0
B_5	-12.50	-21.65	0
B_6	12.50	-21.65	0

Table 2: Co-ordinates of platform connection points

TOP	X	Y	Z
P_1	24.97	-1.31	37
P_2	11.35	22.28	37
P_3	-11.35	22.28	37
P_4	-24.97	-1.31	37
P_5	-13.62	-20.97	37
P_6	13.62	-20.97	37

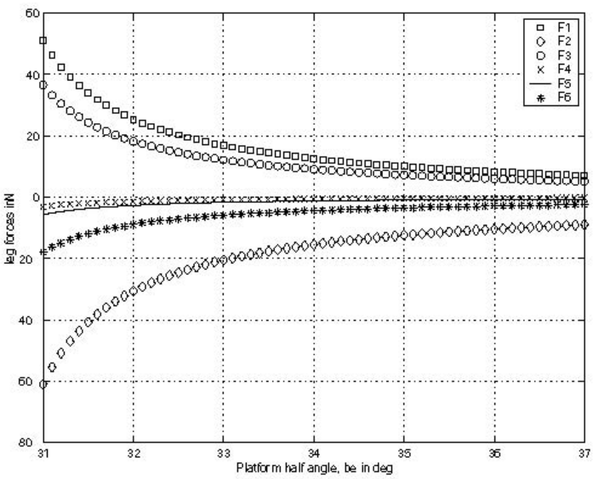

Fig 1b – Leg force variations in a configuration close to singular configurati**on**

Table 3: Sensor specifications

Size of sensor
Diameter =80.0 mm Height = 47.0 mm Thickness of base platform = 5.0 mm Diameter of leg = 12.0 mm
Load Specification
Force along roll axis: Fz (out of plane) = 200 N & sensitivity = 0.5 N
Force along pitch axis: Fx (in-plane) = 50 N & sensitivity = 0.25 N
Force along yaw axis: Fy (in-plane) = 50 N & sensitivity = 0.25 N
Moment about roll axis: Mz = 10000 N-mm & sensitivity = 50 N-mm
Moment about pitch axis: Mx =10000 N-mm & sensitivity = 50 N-mm
Moment about yaw axis: My = 10000 N-mm & sensitivity = 50 N-mm
Materials used
Base & platform – Aluminum alloy: E= 69356.7 N/mm^2; G = 26675.65 N/mm^2 & Poisson's ratio υ = 0.3
Legs & rings – Titanium (Ti-6Al-4V) alloy: E = 109872 N/mm^2, G = 42258.46N/mm^2 & Poisson's ratio υ = 0.3

3.1 Choice of flexible joints in legs

The Stewart platform in its original form has Hook (U) and Spherical(S) joints. In a sensor application, motion at the joints introduces nonlinear effect such as friction, backlash and hysterisis. To avoid these nonlinear effects we use flexible joints. Figure 2 shows two kinds of flexible joints analysed in literature (Paros and Weisboard[6], Ranganath et al.[5]). In our case, we attempted to use the flexible joints shown in Fig. 2b. However, it was observed that for the largest specified loading, the stresses were very high and the joints would fail. Instead the flexure joint type in Fig. 2a was used. The flexure joint used in the sensor is shown in Fig. 3. The main feature of the flexural joint in Fig. 3 is to accommodate rotations about two perpendicular axes by having the thin sections at two different locations perpendicular to each other.

The flexural hinge was modeled in NISA (together with the rest of the sensor) and we performed extensive NISA simulations. The goal was to obtain a design which would not fail for the largest loading and which would satisfy the height specifications.

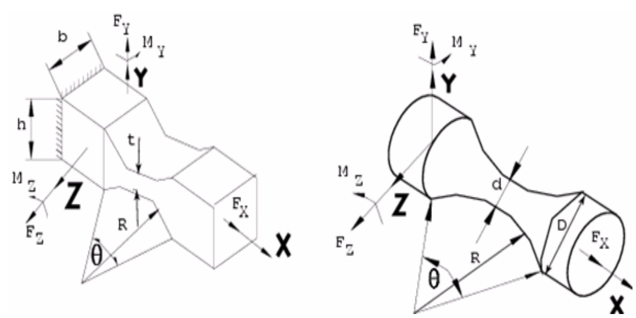

Fig. 2a **Fig. 2b**

Fig 2 – Flexure joints

The key dimensions of the flexural hinge are the leg diameter = 12.0 mm, the flexure length = 3.0 mm and the flexure thickness = 1.5 mm for both axis.

Fig 3 – Flexural hinge used in design

3.2 Design of leg sensing element

In a Stewart platform based force-torque sensor, the prismatic joint is replaced by a sensing element to measure the axial leg force which can be positive or negative. A common approach is to use a proving ring with strain gauges attached to the mid-section of the proving ring. The dimensions of the ring, namely inner and outer diameter, thickness and face width determines the strain at the mid-section. The design of the ring sensing element dimensions should be such that the smallest loading gives at least a measurable strain reading. Further, the design should ensure that for the largest loading, the sensor should not fail. After extensive simulation using NISA, the following dimensions for the ring sensing element shown in Figure 4 have been obtained.

Ring geometry
Outer diameter = 17.25 mm, inner diameter = 14.75 mm
Thickness = 1.25 mm, Face width = 4.0 mm

For this geometry, the strain value for the smallest loading was obtained as 3.2 micro-strains (Table 4b) and is measurable by conventional electronics.

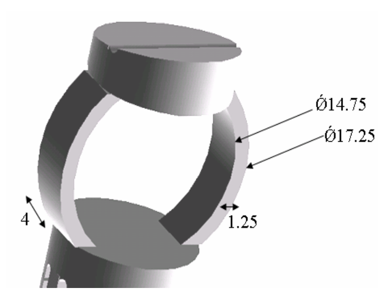

Fig 4 – Ring sensing element

3.3 FE modeling and analysis

With the leg and ring dimensions finalized, the base and platform is chosen to be of 5mm. The full sensor was modeled in NISA and the details of the NISA model are given below.

The finite element model has totally 48400 degrees of freedom. Boundary conditions to the base points at which the sensor is fixed to the ground are assigned zero displacement (Ux = Uy = Uz = 0) & zero rotation boundary conditions (Rx = Ry = Rz = 0). The top & bottom end of the legs are node merged to the platform & base respectively. The shell elements (NKTP = 20) are used to model base, platform & ring. The beam elements (NKTP=12) are used for the legs of the sensor in NISA package.

The strain values in the legs for different loading applied on the FEA model of the sensor are shown in Table 4a. It may be observed that the loading cases were such that they are similar to the ones which are applied during calibration of the sensor in testing shown in Table 5. It is observed that the strain values are significant for moment loads and clearly shows the sensitivity for moments. Further, the strain values for forces are also of a significant magnitude and easily measurable.

Table 4b shows the values strain in each leg for the largest and smallest load. As mentioned earlier, for the smallest load the smallest strain is 3.2 micro-strains. The strain values for the largest load are quite large and we can easily measure them with standard strain gauges and electronics. The maximum stress developed due to the maximum applied load is found to be 465.4 N/mm^2. This shows that the design is safe since the Titanium (Ti-6Al-4V) alloy yields at a stress of 880 N/mm^2 and we get a factor of safety of about 2.0. The first three natural frequencies of the bare sensor with self weight are 496.65, 497.04 and 661.14 Hz about Y, X and Z axis respectively. With a payload mass of 2.3 kg on the platform whose center of mass is about 120 mm from the top of the platform, the first three natural frequencies are found to be 9.22, 9.64 and 19.02 Hz, about Y, X and Z axis respectively. This shows that the sensor is reasonably stiff about the moment axes.

Table 4a – FEM Analysis results

Case	Strain Values in Legs					
	Leg1	Leg2	Leg3	Leg4	Leg5	Leg6
Fx=10 N All other values=0	-149	-24	80	150	65	-122
Fy=10 N All other values=0	8	-157	-125	57	132	100
Fz=9.8N All other values=0	73	64	73	64	73	64
Mx=0.47 Nm All other values=0	-155	122	320	129	-163	-252
My=0.47 Nm All other values=0	-281	-219	-4	216	273	6
Mz=0.47 Nm All other values=0	-86	-118	-86	-117	-87	-117

3.4 CAD models

The force-torque sensor was modeled in UniGraphics and the manufacturing drawings have been made in AutoCAD. The choice of 30-33 half angle combinations make the legs of the Stewart Platform tilted in two planes resulting in two types of legs. The two legs are shown in Figure 5a. Each leg is monolithic in construction and is machined from and is machined from a singe stock of Titanium Ti 6Al 4V alloy. The legs are attached to base and platform by screws. A central hole of diameter 20mm is provided in the top and bottom plates for passage of electrical wire connections. Fig. 5b shows the CAD model of the sensor.

Table 4b – FEM Analysis results for combined loading

	Strain Values in each Leg					
	Leg1	Leg2	Leg3	Leg4	Leg5	Leg6
Max. Load, Fx=Fy=50N, Fz=200N, Mx=My=Mz =10 Nm	-2603	-1441	1588	1797	746	-1625
Min.Load Fx=Fy=0.25 N, Fz=0.5 N, Mx=My=Mz = 0.05 Nm	-14.3	-6.48	6.88	8.44	3.20	-8.84

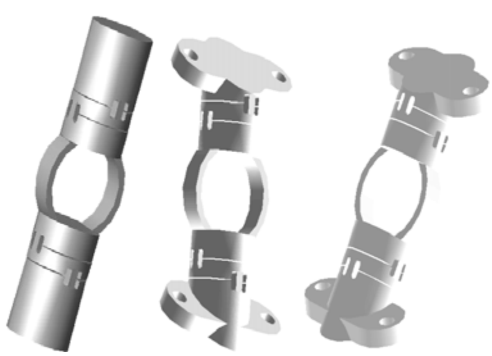

Fig 5a– CAD model of legs

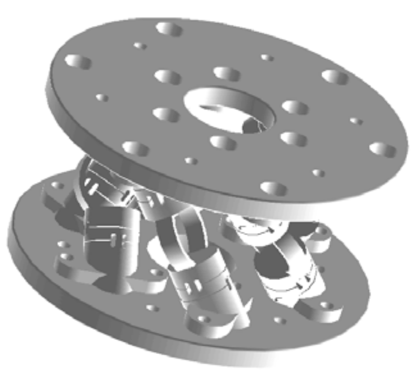

Fig 5b- CAD model of the sensor

4. Instrumentation and assembly

After the fabrication of the legs, strain gauges were mounted in such a way that the gauges are located back to back on the inside and outside surfaces of the sensing rings on the central section of the ring. They are connected in a full bridge configuration in such a way as to get a bridge factor of 4 for better sensitivity. Each of the legs was initially calibrated with dead weights. The typical leg sensitivity is found to be 16 microstrain/N(40 microvolt/N). Subsequently, the legs were assembled with the base and platform at a near-singularity condition taking care to see that excess force is not exerted on any part during assembly. The M3 screws which connect the legs to the base and platform were torqued to 80 Ncm, incrementally at 10 N-cm intervals using torque wrench. The assembled sensor is shown in Fig. 6.

Fig 6 – Fabricated, assembled and instrumented Stewart platform sensor

5. Testing of the sensor

The sensor was calibrated by applying known dead weights incrementally to simulate forces and moments along and about X, Y and Z directions respectively, one at a time, and is shown in Table 5. During the start of each test, standard procedures were carried-out for bridge balancing and the strain values were noted for incrementally applied loads. The loads cases in the calibration tests are similar to that in Table 4a. We observe that the strain values obtained in the legs in the testing are consistently lower in magnitude to that in FEA analysis. This could be due to small variations in dimensions during fabrication of the legs as the flexure dimensions are very sensitive and are in the load path of the sensor. The signs of the microstrains in legs 3 and 6 are different in comparison to that obtained in FEA for My , but it may be noted that these values are very small when compared with that in other legs for the same loading and also the applied moment load is very low and a small fraction of the designed load. Further, it can be clearly noted from the strain values that the sensor is sensitive for the externally applied moments. Further, the forces in X, Y and Z directions are also easily measurable. The behavior of the Leg 1 for different loading corresponding to that in Table 5 is shown in Figs. 7a to 7f and show that the behavior is linear. Table 6 shows the strains in the legs of the sensor for combination loads.

It may be noted from Table 1b that the calibration loading of the sensor is a fraction of the designed loads -- the applied, Fx and Fy, is 20% of the designed load, the Fz applied is about 5% of the designed load and the Mx, My and Mz applied are about 5% of the designed load. The calibration of the sensor for full loads requires different test setup and will be taken-up shortly. Nevertheless one can see that the microstrain values obtained for external forces are easily measurable. The microstrains measured are large for applied moments in comparison to applied forces in terms of percentage of designed load, thus clearly indicating higher sensitivity to moments.

From Table 5, it is seen that the results of calibration at low loads are very encouraging from a viewpoint of sensitivity to applied moments and also measurability to applied forces. The derivation of the transformation matrix, which is essential for measuring unknown external forces and moments on the sensor, will be obtained after testing with full loading and more detailed tests.

Table 5 – Calibration of the sensor

Case	Strain Values in Legs					
	Leg1	Leg2	Leg3	Leg4	Leg5	Leg6
Fx=10 N All other values=0	-87	-16	37	110	54	-77
Fy=10 N All other values=0	4	-89	-93	38	83	60
Fz=9.8N All other values=0	62.	11	63	42	22	59
Mx=0.47 Nm All other values=0	-94	92	222	47	-133	-173
My=0.47 Nm All other values=0	-177	-148	8	158	201	-5
Mz=0.47 Nm All other values=0	-23	-66	-49	-55	-41	-77

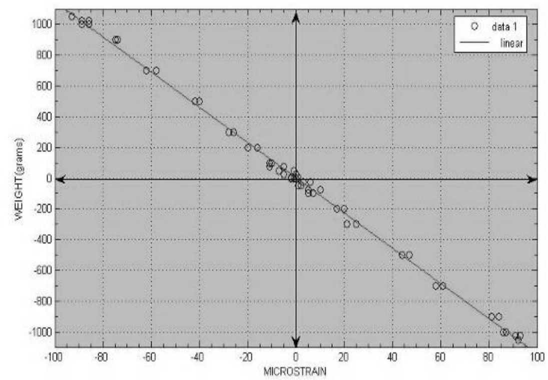

Fig. 7a Strain variation in Leg1 for Fx

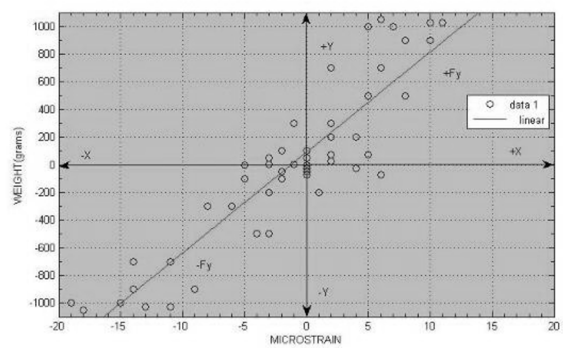

Fig. 7b Strain variation in Leg1 for Fy

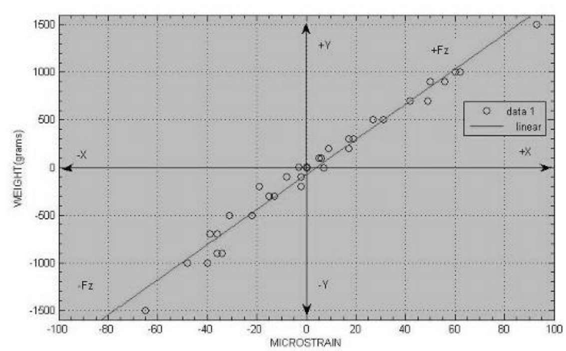

Fig. 7c Strain variation in Leg1 for Fz

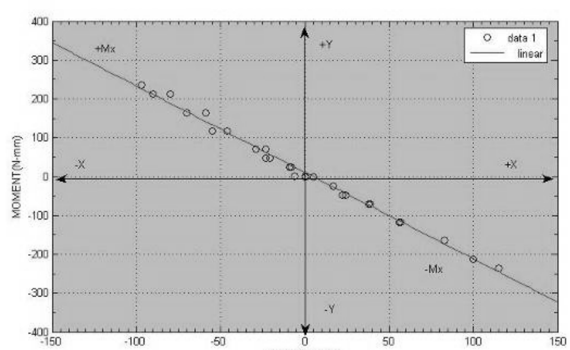

Fig. 7d Strain variation in Leg1 for Mx

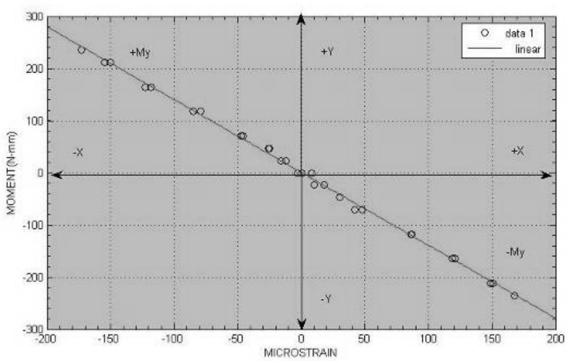

Fig. 7e Strain variation in Leg1 for My

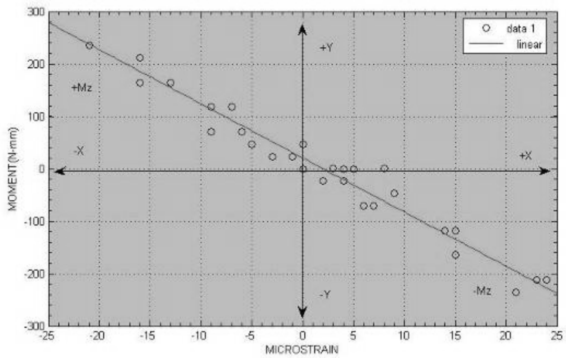

Fig. 7f. Strain variation in Leg1 for Mz

Table 6: Micro-Strain for combined loadings

Sl. No	Load Force (N) Moment(Nm)	Microstrains in legs					
		L1	L2	L3	L4	L5	L6
1	Fx=4.9, Fy=Fz=0, Mx=My=Mz= -0.117	-39	86	10	78	64	-37
2	Fx=4.9, Fy=4.9 Fz=0, Mx=My=0, Mz=- 0.235	-28	86	-36	66	37	-49
3	Fx=4.9, Fy=4.9, Fz=- 2.94, Mx=0,My=- 0.07,Mz=- 0.235	-59	85	-62	80	32	-83
4	Fx=4.9N, Fy=4.9N Fz=-5.88N, Mx=0.07 Nm, My=-0.07Nm, Mz=-0.235 Nm	-70	-92	-51	86	34	-89

6. Conclusions

In this paper, we have described the configuration selection, design and initial experimental results of a Stewart platform based six axis force-torque sensor in a near-singular configuration which is sensitive for externally applied moments. From the given specification, we first chose a configuration which has enhanced sensitivity for the externally applied moment components. The joints have been replaced by flexural hinges and the ring shaped strain sensing element has been introduced in the legs for measuring forces in the legs.

FEA simulations in NISA have been carried out on the sensor to ensure that the designed sensor met the required specifications. The sensor has been fabricated in GT&TC Bangalore. The preliminary testing has been done for various loading conditions at ISAC-ISRO, Bangalore. The results of the preliminary tests are encouraging and show a marked sensitivity to external moments. The full scale testing and derivation of the transformation matrix is underway.

Acknowledgement

The authors sincerely thank Indian Space Research Organisation and Space Technology Cell (Indian Institute of Science, Bangalore) for funding the research and development of this sensor.

References

[1] Gorinevsky, D. M., Formalsky, A. M., and Schneider, A. Y., "Force Control of Robotics Systems," CRC Press, New York, 1997.

[2] Stewart, D., "A platform with six degrees of freedom, Proc. of Institution of Mechanical Engineers," Part 1, Vol. 180(15), 1965, pp. 371-386.

[3] Gaillet, A. and Reboulet, C., "A isostatic six component force and torque sensor, Proc. of the 13 Int. Conf. On Industrial Robotics," 1983, pp. 8.102-18.111.

[4] Dwarakanath, T. A., Dasgupta, B. and Mruthyunjaya, T. S., "Design and development of a Stewart Platform based force-torque sensor," Mechatronics, Vol. 11, 2001, pp. 793-809.

[5] Ranganath, R., Nair, P. S., Mruthyunjaya, T. S., and Ghosal, A., "A force-torque sensor based on a Stewart Platform in a near-singular configuration", Mechanism and Machine Theory, Vol. 39, Sept., 2004, pp. 971- 998 .

[6] Paros, J. M. and Weisbord, L., "How to design flexure hinges," Machine Design, 1965, pp. 151-156.

[7] Dasgupta, B., "The Stewart Platform Manipulator: Dynamic Formulation, Singularity Avoidance and Redundancy, "Ph.D. thesis, IISc, 1996.

[8] Ranganath, R., "Analysis and design of a Near-Singular Stewart platform Based Force-torque Sensor," Ph.D. thesis, IISc, 2002.

[9] M. Prashanth, Shivanand Bhavikatti, R. Ranganath and A. Ghosal., "Analysis and design of a moment sensitive flexure jointed Stewart Platform based force-torque sensor in a near-singular configuration," Proc.of 5th National Seminar on Aerospace and Related Mechanisms , ISRO Satellite Centre, Bangalore, Nov. 2005, pp. 221-226 .

[10] Sorli, M., and Pastorelli, S., "Six-axis reticulated structure force/torque sensor with adaptable performances," Mechatronics, Vol. 5, No.6, 1995, pp. 585-601.

[11] Champagne, P. J., Cordova, S.A., Jacoby, M.S., and Lorrel, K.R., "Development of a precision laboratory dynamometer," NASA-CP-3147, 26TH Aerospace Mechanisms Symposium, 1992, pp. 331-348.

[12] Fichter, E.F., "The Stewart platform manipulator : general theory and practical construction," International Journal of Robotics Research, Vol. 5(2), 1986, pp.157-182.

[13] McInroy , J. E., and Hamaan , J. C., "Design and control of flexure jointed hexapods," Vol. 16, No.4, pp. 372-381, 2000.